An Experimental Study on Fouling over a Single Tube

Man Yeong Ha,* Dae Rae Lee,* Seung Phyo Ahn* and Ho Dong Park*

(*Received October 20, 1997*)

An experimental study to investigate the fouling phenomena over a single tube is carried out in the hot wind tunnel. The temperature of gas and cooling air, and the temperature in the fouling probe are measured as a function of time, probe position, gas temperature, particle feeding rate, cooling air flow rate, etc., giving the local and average heat transfer rate and fouling factor. The amount of foulant adhered to the probe has different values at the different positions on the probe surface, giving different heat transfer rate and fouling factors as a function of position on the probe surface. The fouling factor increases with the flow rate of cooling air and foulant feeding rate. The local fouling factor increases with the gas temperature but the average fouling factor does not depend much on the gas temperature above 700°C.

Key Words: Fouling, Heat Transfer, Experimental Study, Particulate Two-Phase Flow

Nomenclature

A : Surface area
C_p : Specific heat
d : Diameter
h : Heat transfer coefficient
k : Thermal conductivity
L : Length
$\dot{m}_a$: Mass flow rate of cooling air
$\dot{m}_p$: Particle feeding rate
$\dot{Q}$: Heat transfer rate
R_f : Fouling factor
T : Temperature
U : Overall heat transfer coefficient

subscript

a : Air
avg : Average
c : Clean
f : Fouling
g : Gas
i : Inside, inlet
$local$: Local
o : Outside, outlet
rc : Radiative-convective
wi : Inside wall

* School of Mechanical Engineering Pusan National University San 30, Jangjeon-Dong, Kumjung-Ku Pusan 609-735 Korea

1. Introduction

One of the most difficult problems experienced in the initial design and during operation of utility boiler is fouling phenomena due to the fly ash generated by coal firing. The fouling by fly ash on the surface of heat exchanger is a primary factor to decrease the performance of utility boiler, causing an enormous energy loss and increasing the cost for maintenance and reconstruction. The fouling process consists of an initial delay period, particulate transfer to the heat exchanger surface, deposition, aging, removal and re-deposition. During the initial time delay period, the conditions to initiate the fouling process are formed on the surface of heat exchanger. The heat transfer rate during the initial period increases a little bit because the roughness formed by initial particulate deposition destroys the boundary layer. The initial time delay period can or can't exist depending on operating conditions. According to the previous studies (Nbeal, 1970, Wenglarz, 1981, Lister, 1981, Ha et al., 1996, Lee et al., 1997), Brownian diffusion, thermophoresis, inertial impaction, turbulent diffusion, gravity, electro-magnetic fields, etc., are important mechanisms to transport the foulants to

the wall. If the particulate deposition process starts, physical and chemical changes occur on the surface of heat exchanger. The removal of the foulants deposited on the wall occurs due to the erosion, thermal dissociation and gravity fall. The fluid velocity is one of the most important parameters to affect the fouling behavior. With increasing the fluid velocity, the particulate deposition and removal by erosion increase and the net effect is the thickness derease of the foulants deposited on the wall. Thus the fouling factor decreases with increasing the fluid velocity. The fluid temperature affects the chemical reaction rate, crystallization rate and polymerization, giving the increasing fouling with fluid temperature (Gdmundson, 1981). The wall temperature affects the crystallization rate and the strength of the particulate deposition adhered to the wall. The particulate deposition adhered to the surface of a heat exchanger grows in the opposite direction to the fluid flow direction and is consisted of inner, intermediate and outer layers which determine the fouling characteristics. Thus the structure of each layer and its effect on the fouling should be investigated.

Borio et al (1977) investigated the slagging and fouling properties using the pilot scale solid fuel burning test facility. They developed a standardized test procedure giving a highly quantitative chemical, physical, and thermal property measurements to be determined on ash deposits as a function of firing rate, providing the designer with information concerning relative ash deposition rates, critical gas temperatures, relative deposit bonding strengths, and relative waterwall heat absorption rates. Barratt and Unsworth (1988) investigated the chemical and physical structure of ash deposits formed on the surface of heat exchanger during combustion of a number of pulverized coals in a pilot scale combustor under conditions similar to those in a utility boiler furnace. They also investigated the strength of ash deposits by blowing soots by air lance. Baxter et al. (1990) investigated dynamic growth of ash deposits using the high speed cameras and the temperature controlled deposition probes in the multifuel combustor, and carried out experiments at conditions simulating three locations (near -flame region, the superheater region, and the convection pass) in a boiler. The results showed the particle capture efficiencies and the fraction of fly ash particles that adhered to the probe upon contact as a function of coal type, extent of particle burnout, and time.

Marner and McDavid (1989) developed a fouling probe to monitor the fouling process. They injected slaked lime into the hot gas stream formed by gas firing and observed the shape of particles deposited on the fouling probe, presenting the local and average fouling factor as a function of gas temperature, gas velocity, flow rate of cooling air, etc. Sohal (1993) applied the similar fouling probe with a microprocessor -based control system and a data acquisition system to the industrial flue environment at two utility boiler sites, and proved that the probe was capable of measuring fouling in a harsh environment. He also suggested several improvements to the probe to further increase its capabilities to monitor fouling effects in varied environments. Kamer et al. (1994) suggested the new analysis techniques using the scanning electron microscopy and the electron microprobe analysis (SEM/EMPA) in order to understand deposit formation mechanisms and to help control boiler fouling.

Reid (1984) and Walsh et al. (1990) explained the effects of mineral composition of coal ash on the particle deposition on the surface of heat exchangers in their review paper. Baxter and Desollar (1993) and Walsh et al. (1992) suggested the theoretical model to calculate the growth of particles deposited on the heat exchanger surface. They included the effects of inertial impaction, thermophoresis, condensation, chemical reaction, etc. in their model. Even though their model is not fully verified by the experimental data at pilot and utility scales, their results can be used to predict the qualitative trends of fouling phenomena.

The behavior of gas flow and fly ash motion has an important effect on the performance of utility boiler using the coal as a fuel. However, many researches were not carried out due to the

difficulties in the experiments and the very complex phenomena of particulate two-phase flow. Thus, in the present study, we designed the hot wind tunnel to reproduce the conditions of utility boiler and carried out its performance test. We introduce the temperature control system in the test section. The foulants are injected into the hot gas stream through the particle feeding system including particle generating system. The particulate two-phase flow behaviour, the fouling and heat transfer characteristics to the heat exchanger are investigated as a function of gas temperature, fouling probe position, particle feeding rate, flow rate of cooling air.

2. Experimental Equipments and Methods

Figure 1 shows a drawing of hot wind tunnel used in the present study. The total length is 10. 78m and the height is 2m. Each section is connected with flanges. The major components of the hot wind tunnel are the combustion system, temperature control part, particle generation system, foulant injection part, contraction section, test section and chimney. The wall of hot wind tunnel is insulated with refractory materials.

The combustor generates hot gas flame whose length and width are about 2 and 0. 7m, respectively. The burner uses oil as a fuel with the flow rate of 110l/h. The diameter and length of the combustor are 1 and 2m, respectively. The flow rate of fuel is proportional to that of air which is controlled by opening and closing butterfly valve operated by the control motor automatically or manually. The air supplied by the blower is divided into the air for fuel injection and that for combustion. The flow rate of air for fuel injection and combustion is controlled automatically by the air control valve. The combustor changes its shape from a circle to a rectangular at the exit with decreasing cross sectional area because the cross section of the hot wind tunnel has a rectangular shape.

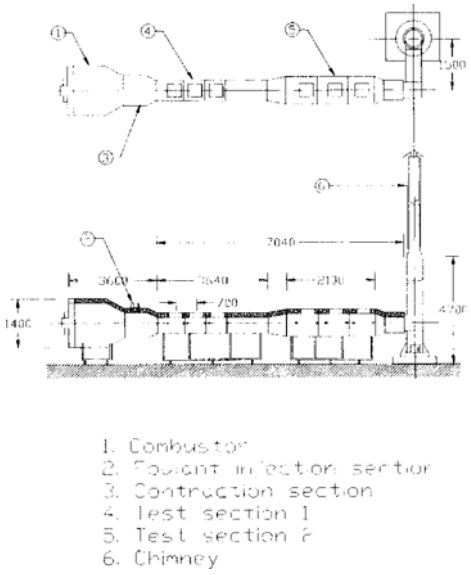

Fig. 1 A drawing of hot wind tunnel.

The foulant injection section follows the combustor. This section has a rectangular cross section and its length is 0.8m. Calcium hydroxides with particle size distribution shown in Fig. 2 is used as foulant in the present experiment. The foulant is stored in the storage tank and the agitator in the storage tank is rotated to prevent the agglomeration of the foulants. The foulants are transferred to the hopper through the screw feeder and fall down by gravity. The vacuum pump at the bottom of the hopper sucks in the foulants. The foulants is feeded into the hot wind tunnel by compressed air. The feeding rate of the foulant is determined by the revolution speed of the screw feeder. The R-type thermocouple for PID control of gas temperature is located very close to the foulant injection hole. The R-type thermocouple for PID temperature control measures the hot gas temperature.

The contraction section follows the foulant

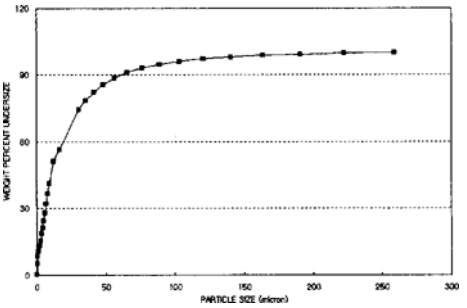

Fig. 2 Particle size distribution.

injection section. This section is used to obtain the uniform flow velocity in the test section and has a three-dimensional curved shape with the contraction rate of 4 and is designed according to the Morel's method of Tulapurkara and Bhalla (1988).

The test section follows the contraction section and consists of two parts in order to see the effect of gas velocity on the fouling. The cross-sectional area in the second part of test section is twice as much as that in the first part, reducing the flow velocity half of that in the first part. The first part has three ducts whose cross sections are 0.3m×0.3m and whose length is 0.9, 0.7, and 1.14m, respectively. These ducts are connected by the flange. The second part also has three ducts whose cross sections are 0.45m×0.45m and lengths are 0.7m. The six lids are located at the upper part of test section and each lid is made a single body with a fouling probe. The fouling probe is a single tube or tube bundles with staggered or non-staggered configuration depending on the experimental conditions. The side part of the test section has holes of $\phi 33$ and insert the measuring probes such as thermocouples, pitot tube, etc., through this hole. More detail informations for experimental equipments are shown by Ha and Kim (1997).

Figure 3 shows the assembly of fouling probe used in the present experiment. The fouling probe used is the Cr-Mo steel used in the utility boiler. The K-type thermocouple is used to measure the temperature at the inner and outer surface of the fouling probe. Because the fouling probe is exposed to the hot gas stream, the cooling air passes through inside of the fouling probe in order to control the fouling probe temperature.

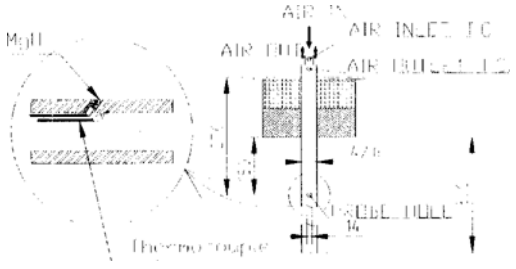

Fig. 3 Assembly of fouling probe.

The cooling air is supplied by the blower or compressor. If we change the flow rate of cooling air, we can control the temperature at the inner and outer surface of the fouling probe which is one of the important factors to affect the fouling behavior. The temperatures of cooling air at the inlet and exit are measured using the K-type thermocouple.

The data acquisition system measures the gas temperature before and after the fouling probe, the temperature at the inner and outer surface of the fouling probe, and the cooling air temperatures in order to calculate the heat transfer rate and fouling factor while the foulants are adhered to the fouling probe. All temperatures are recorded as a function of time using the computer. The pitot tube with circulating cooling water measures the gas velocity exposed to the hot gas stream. The gas velocity measured using the pitot tube of the present study is compared with that using the commercial pitot tube in the cold flow condition in order to check the accuracy of the measured gas velocity using the present pitot tube, representing well in the cold flow condition. The hot gas velocity measured using the present pitot tube is corrected by compensating the density in the hot flow condition.

We calculate the local and average fouling factor using the measured data and similar calculation method given by Marner and MacDavid (1989). The local heat transfer rate at the stagnation point from the hot gas to the probe is calculated as

$$Q_{local} = UA_0 \Delta T = UA_0 (T_g - T_{wi}) \tag{1}$$

where A_0, T_g and T_{wi} are the outside surface area of the probe, gas temperature and inside wall temperature, respectively. U in Eq. (1) represents the overall heat transfer coefficient. Thus, the thermal resistance, $\left(\frac{1}{U}\right)_c$, under clean conditions before particulate deposition may be expressed as

$$\left(\frac{1}{U}\right)_c = \frac{1}{h_{rc}} + \frac{A_0 \ln (d_0/d_i)}{2\pi k L} \tag{2}$$

where h_{rc} represents the convective-radiative heat transfer coefficient between the probe and hot gas. d_i, d_0, L and zp in Eq. (2) are, respectively, the

inside diameter, outside diameter, length and thermal conductivity. The thermal resistance, $\left(\frac{1}{U}\right)$, with fouling after particulate deposition may be expressed as

$$\left(\frac{1}{U}\right)_f=\frac{1}{h_{rc}}+\frac{A_0\ln(d_0/d_j)}{2\pi kL}+R_f \tag{3}$$

where R_f represents the fouling factor. Thus the local fouling factor at the forward stagnation point is calculated using Eqs. (2) and (3) expressed as

$$(R_f)_{local}=\left(\frac{1}{U}\right)_f-\left(\frac{1}{U}\right)=\left(\frac{A_0(T_g-T_{wi})}{\dot{Q}_{local}}\right)_f-\left(\frac{A_0(T_g-T_{wi})}{\dot{Q}_{local}}\right)_c \tag{4}$$

$\dot{Q}_{local}$ in Eq. (4) is calculated using the inside and outside temperature measured for the case with and without fouling expressed as

$$\dot{Q}_{local}=\frac{T_{wo}-T_{wi}}{\frac{\ln(d_0/d_j)}{2\pi kL}} \tag{5}$$

The average fouling factor is calculated using the inlet and outlet temperatures measured for cooling air, $T_{a,j}$ and $T_{a,o}$, expressed as

$$(R_f)_{avg}=\left(\frac{1}{U}\right)_f-\left(\frac{1}{U}\right)_c=\left(\frac{A_0LMTD}{\dot{Q}_{avg}}\right)_f-\left(\frac{A_0LMTD}{\dot{Q}_{avg}}\right)_c \tag{6}$$

where Q_{avg} and $LMTD$ in Eqs. (6) are expressed as

$$\dot{Q}_{avg}=\dot{m}_aC_{pa}(T_{a,o}-T_{a,j}) \tag{7}$$

$$LMTD=\frac{(T_g-T_{a,o})-(T_g-T_{a,j})}{\ln\left(\frac{T_g-T_{a,o}}{T_g-T_{a,j}}\right)} \tag{8}$$

3. Results and Discussion

The experiment starts by igniting the burner and setting up the target temperature in the test section. We monitor the gas temperature measured from the thermocouple for PID temperature control located before the contraction section and wait for until the gas temperature reaches the target temperature. It takes more than a hour for the gas temperature in the test section to reach the

Table 1 Parameters used in the present experiment.

Parameter	Range
Gas Temperature, T_g	700~1000 ℃
Average Gas Velocity, V_g	8~10 m/s
Test Duration, t	2~3 hours
Particulate Feed Rate	33.23~44.39 g/min
Cooling Air Feed Rate	0.0168~0.0451 m³/s

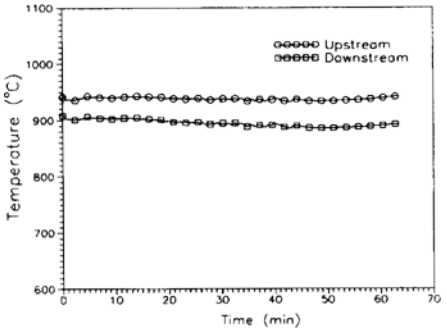

(a)

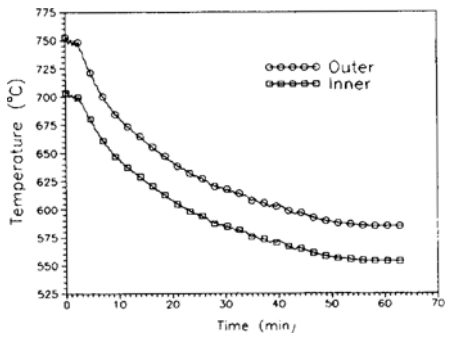

(b)

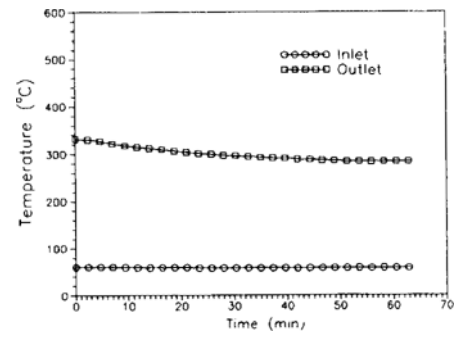

(c)

Fig. 4 Typical data for (a) gas temperature, (b) probe surface temperature and (c) cooling air temperature as a fuction of temperature: T_g= 100°C, V_g=8 m/s, $\dot{Q}$=0.0168 m³/s, dpa $_p$= 44.39 g/min.

steady state of the target temperature. After the system reaches the steady state, the foulants generated in the particle generation system are injected into the hot gas stream. Table 1 shows the parameters used in the present experiment to study the heat transfer and fouling under different experimental conditions. These parameters give Reynolds numbers in the range of 1870~3620 based on the fouling probe diameter, gas velocity and kinematic viscosity.

Figure 4 shows the typical data for gas, surface and cooling air temperature as a function of time. These are measured at the upstream and downstream of fouling probe, at the inner and outer surface of stagnation point of fouling probe, at the inlet and outlet of fouling probe, respectively. These temperatures are used to calculate the heat transfer rate and fouling factors in Eqs. (1) ~ (8). The gas temperature maintains almost the steady state during the experiment after the system reaches the steady state. With the particle feeding, the value itself of the inner and outer surface temperature and the difference between the inner and outer surface temperature decrease with increasing amount of particle adhered to the probe surface as time goes by. The inlet temperature of cooling air maintains a constant value but the outlet temperature decreases with particle deposition on the probe similar to the surface temperature. The gas, surface and cooling air temperature data obtained from the present experiments for the following cases are shown by Ha and Kim (1996).

At the end of the experiment, we take the fouling probe out of the test section, observe the shape and measure the thickness of foulant deposited on the surface of fouling probe. Figure 5 shows the sketch of the typical shape of particles deposited on the fouling probe. Figure 6 shows a photo for the fragment of foulants adhered around the stagnation point. The particulate deposition pattern, heat transfer and fouling factor along the probe have close relation with the gas flow over the fouling probe. The particulate two-phase flow impinges directly on the stagnation point, leaving the large amount of foulants adhered to the stagnation point ($\theta=0°$) of the

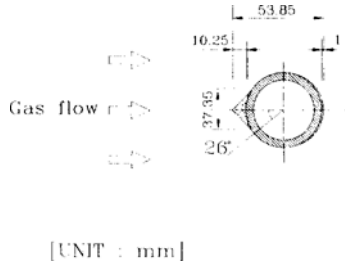

Fig. 5 A typical shape of particle deposited on the surface of fouling probe.

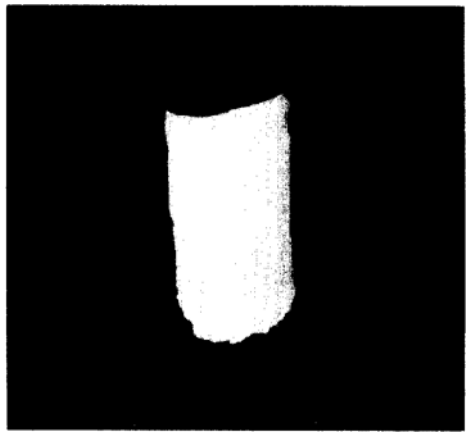

Fig. 6 A fragment of particle deposited around the stagnation point of fouling probe.

fouling probe. The stagnation point is the location of maximum pressure. The pressure decreases in the stream-wise direction and the particulate two-phase flow accelerates under the influence of a favorable pressure gradient. The foulant adhered to the probe is removed and entrained to the gas flow due to erosion, giving decreasing thickness in the stream-wise direction from the stagnation point. Thus, the particles are little deposited on the probe surface around $\theta=90°$, which maintains relatively clean condition. After a pressure eventually reaches a minimum value, the flow decelerates toward the rear of the probe in the presence of an adverse pressure gradient, leading to flow separation and formation of a wake in the downstream region. Thus the foulant is re-entrained in the wake region again and adhered to the probe around $\theta=180°$. The physical characteristics of foulants adhered to the stagnation point around $\theta=0°$ shows a high cohesive power with the smooth surface. But the foulants

adhered in the wake region around $\theta=180°$ show very low cohesive power and are detached easily with small disturbance.

The heat transfer rate and fouling factor for different positions along the probe from the stagnation point are investigated as a function of time. In order to measure the temperature at the inner and outer surface for different positions of $\theta=0°$ (stagnation point), 90° and 180°, the experiments are carried out separately after the assembly of fouling probe is first located in the position normal to the flow direction and then rotated in the clockwise direction of 90° and 180°. The target gas temperature, gas velocity, flow rate of cooling air and foulant feeding rate are 1000°C, 8 m/s, 0.0282 m³/s and 44.39 g/min, respectively.

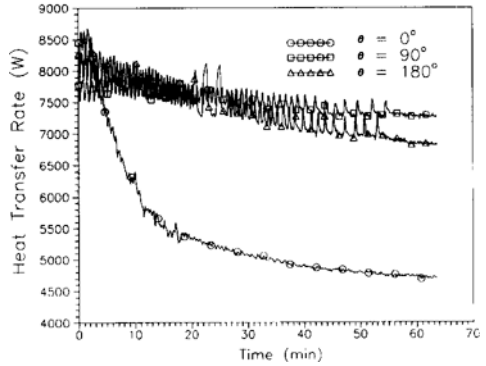

Fig. 7 Local heat transfer rate for different angles of $\theta=0°$, 90° and 180° as a function of time: $T_g=1000$ °C, $V_g=8$ m/s, $\dot{Q}=0.0282$ m³/s, $\dot{m}_p=44.39$ g/min.

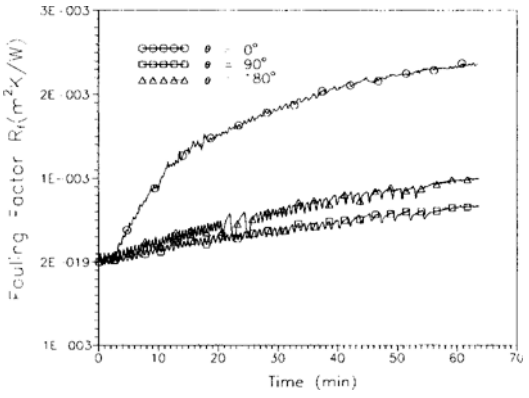

Fig. 8 Local fouling factor for different angles of $\theta=0°$, 90° and 180° as a function of time: $T_g=1000$ °C, $V_g=8$ m/s, $\dot{Q}=0.0282$ m³/s, $\dot{m}_p=44.39$ g/min.

Figures 7 and 8 show the local heat transfer rate and fouling factor for different positions of $\theta=0°$, 90° and 180° as a function of time. The circle, square and triangle in Figs. 7 and 8 represent the heat transfer rate and fouling factor at $\theta=0°$, 90° and 180°, respectively. The heat transfer rate decreases and fouling factor increases with increasing foulant deposition since the thermal resistance increases due to fouling. Because the thermal conductivity of foulant is low compared to that of probe, the heat transfer rate decreases and fouling factor increases very rapidly once the foulant is adhered to the fouling probe. The decreasing rate of the local heat transfer rate and increasing rate of the fouling factor during an initial period with foulant feeding is very large when a large amount of foulant is adhered to the surface of probe. As time goes by, the amount of foulant adhered to the fouling probe reaches the equilibrium state with that removed from the fouling probe, giving almost the uniform foulant deposition. Thus, the heat transfer rate decreases and fouling factor increases gradually, approaching to the steady state of uniform value. Before the foulant feeding, the local heat transfer rate at $\theta=0°$ has a maximum value. The local heat transfer rate decreases in the streamwise direction, giving lower value at $\theta=90°$ compared to that $\theta=0°$. The heat transfer rate increases slightly again in the wake region, resulting in the larger heat transfer rate at $\theta=180°$ compared to that at $\theta=90°$. After the foulants are injected into the hot gas stream, the foulants are adhered to the probe. The amount of foulants adhered to the probe has a maximum value at the stagnation point of $\theta=0°$. The local heat transfer rate and fouling factor at $\theta=0°$ decrease very rapidly during an initial period, followed by slowly decreasing period and approaching to the final steady state. However, because the amount of foulants adhered to the probe at $\theta=90°$ and 180° is very small compared to that at $\theta=0°$, the local heat transfer rate at $\theta=90°$ and 180° decrease gradually compared to that at $\theta=0°$, giving larger heat transfer rate and smaller fouling factor at $\theta=90°$ and 180° compared to those at $\theta=0°$. The local heat transfer rate

at $\theta=90°$ is larger than that at $\theta=180°$ and the fouling factor at $\theta=90°$ is smaller than that at $\theta=180°$ since the thickness of foulants adhered to the probe at $\theta=90°$ is smaller than that at $\theta=180°$.

Figure 9 shows the average fouling factor as a function of time when the assembly of fouling probe is located at the normal direction ($\theta=0°$) to the hot gas flow and rotated in the clockwise direction of $\theta=90°$ and 180° from the stagnation point. The average fouling factor without foulant feeding is zero since the surface of fouling probe is clean. The fouling factor increases rapidly during the initial period of foulant feeding. As time goes by, the fouling factor increases gradually and approaches to the constant value, meaning that the adhesion and removal of foulants reach an equilibrium state. Thus, the curve of fouling factor shows an exponential shape. At the end of this experiment after one hour with foulant feeding, the fouling factor increases very gradually as shown in Fig. 9. Thus, one hour is not enough time to reach an equilibrium state for adhesion and removal of foulants. The average fouling factor should be the same irrespective of the position of fouling probe in the flow direction of hot gas under the same experimental condi-

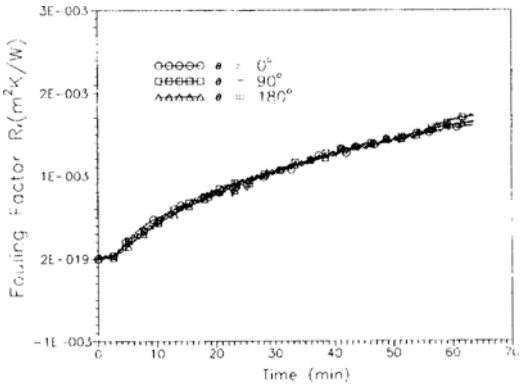

Fig. 9 Average fouling factor for different angles of $\theta=0°$, 90° and 180° as a function of time: $T_g=1000$ °C, $V_g=8$ m/s, $\dot{Q}=0.0282$ m³/s, $\dot{m}_p=44.39$ g/min.

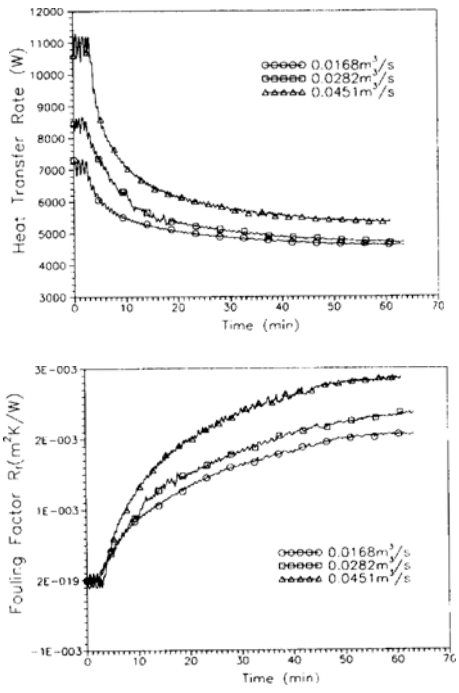

Fig. 10 Local heat transfer rate and fouling factor for different flow rates of cooling air as a function of time: $T_g=1000$ °C, $V_g=8$ m/s, $\dot{m}_p=44.39$ g/min.

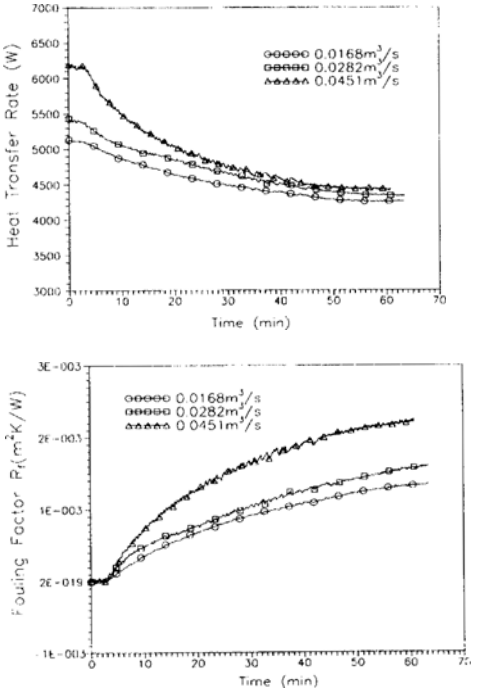

Fig. 11 Average heat transfer rate and fouling factor for different flow rates of cooling air as a function of time: $T_g=1000$ °C, $V_g=8$ m/s, $\dot{m}_p=44.39$ g/min.

tions. The average fouling factor shown in Fig. 9 is almost the same for different positions of probe, showing the reproducibility of the present experiment.

Figure 10 shows the local heat transfer rate and fouling factor at the stagnation point as a function of time for different flow rates of cooling air. The target gas temperature, gas velocity and foulant feeding rate are 1000°C, 8 m/s and 44.39 g/min, respectively. The flow rate of cooling air used are 0.0168, 0.0282 and 0.0451 m^3/s, respectively. The flow rate of cooling air can control the surface temperature of probe. With increasing flow rate of cooling air, because the probe surface temperature itself decreases and the temperature difference between the gas and the probe surface increases, the local heat transfer rate increases with flow rate of cooling air. We may postulate that the conditions for foulants to be condensed on the probe surface can be easily formed under the conditions of decreasing probe surface temperature. With increasing flow rate of cooling air, the amount of foulants adhered to the probe surface increases, giving increasing thickness and width of foulant deposition around the stagnation point. The decreasing rate of local heat transfer rate during an initial period increases with increasing flow rate of cooling air. The slope of decreasing rate of heat transfer rate determines the fouling factor. Thus the local fouling factor increases with flow rate of cooling air due to increasing foulant deposition on the probe surface. Figure 11 shows the average heat transfer rate and fouling factor as a function of time for different flow rates of cooling air. Because the average thickness of foulants adhered on the probe is smaller than the thickness at the stagnation point, the values of average heat transfer rate and fouling factor is lower than the local values at the stagnation point, but the variation of average heat transfer rate and fouling factor is similar to the local ones, giving increasing values with flow rate of cooling air.

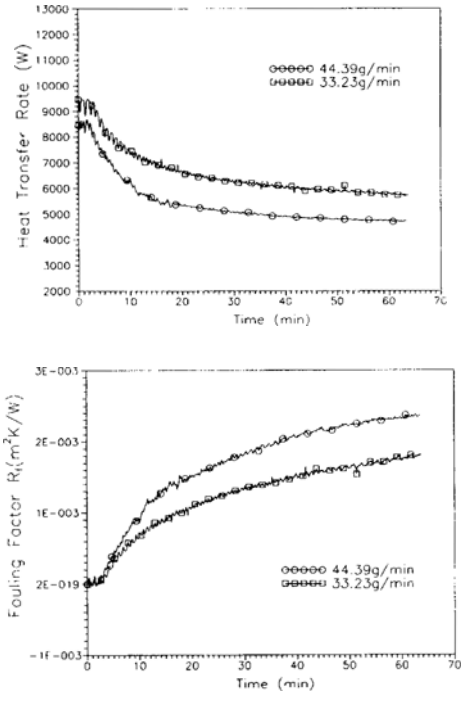

Fig. 12 Local heat transfer rate and fouling factor for different foulant feeding rate as a function of time: $T_g=1000$ °C, $V_g=8$ m/s, $\dot{Q}=0.0282$ m^3/s.

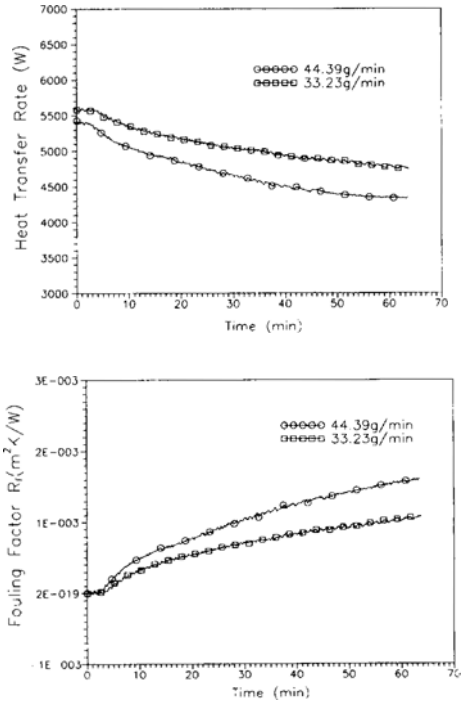

Fig. 13 Average heat transfer rate and fouling factor for different foulant feeding rate as a function of time: $T_g=1000$ °C, $V_g=8$ m/s, $\dot{Q}=0.0282$ m^3/s.

If the feeding rate of foulant increases, the foulant concentration in the gas stream and the amount of foulant deposition on the probe increase. The thickness and width of foulant adhered around the stagnation point for the foulant feeding rate of 37.05 g/min are 9.25 and 37.05 mm, respectively, and those for the foulant feeding rate of 44.39 g/min are 11.3 and 39.85 mm, respectively. Figure 12 shows the local heat transfer rate and fouling factor and Fig. 13 shows the average ones as a function of time for different foulant feeding rates of 33.23 and 44.39 g/min. Because the amount of foulants adhered to the probe surface increases with foulant feeding rate, the decreasing rate of heat transfer rate increases with feeding rate of foulant feeding, giving increasing fouling factor.

Figure 14 shows the local heat transfer rate and fouling factor and Fig. 15 shows the average ones as a function of time for different gas temperatures. If the gas temperature increases, the difference between the gas and surface temperature increases and the heat transfer rate increases. The decreasing rate of heat transfer is governed by the foulant deposition and determines the fouling factor. The decreasing rate of local heat transfer rate for the target gas temperature of 1000 °C is larger than that for 700 °C and has similar values to those for 850 °C. Thus the local fouling factor for the target gas temperature of 1000 °C shows bigger values than that for 700 °C and has similar values to that 850 °C. For the average heat transfer rate, the decreasing rates of heat transfer rate for the target gas temperature of 700, 850 and 1000 °C show the similar values. Thus the average fouling factor as a function of time has the similar values as shown in Fig. 15. There exists the condition of critical gas temperature for the foulants to be adhered to the probe surface. Below this critical temperature, the foulant is dry and the amount of foulant to be deposited on the probe surface is very small. However, above this critical

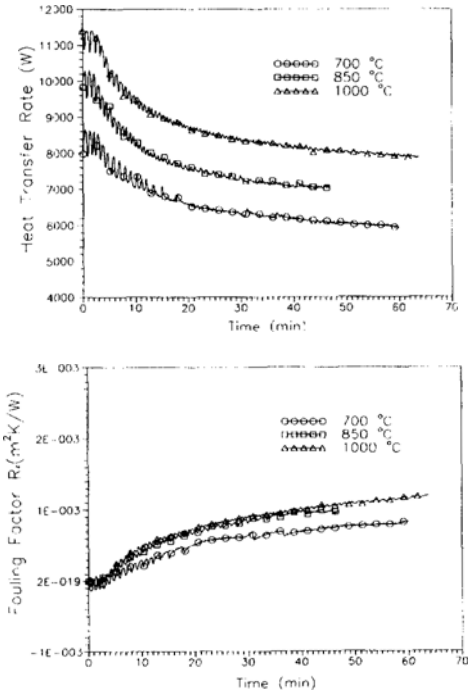

Fig. 14 Local heat transfer rate and fouling factor for different target gas temperature as a function of time: $V_g=8$ m/s, $\dot{Q}=0.0282$ m³/s, $\dot{m}_p=44.39$ g/min.

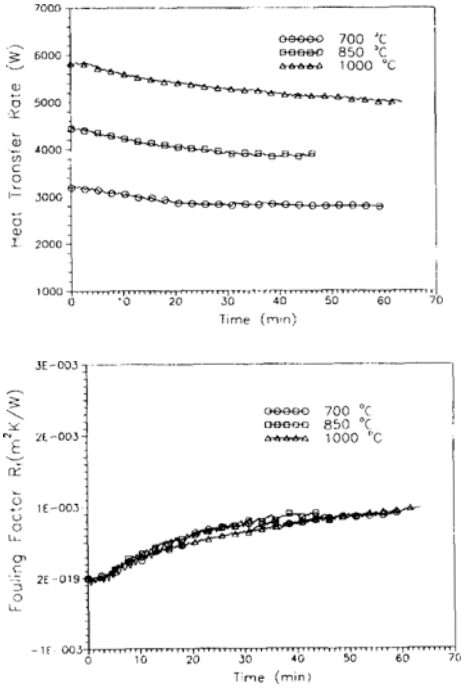

Fig. 15 Average heat transfer rate and fouling factor for different target gas temperature as a function of time: $V_g=8$ m/s, $\dot{Q}=0.0282$ m³/s, $\dot{m}_p=44.39$ g/min.

temperature, sticky particles can be formed in the foulants and the amount of foulant deposition increases. The value of critical gas temperature depends on the kind of foulants. In the present experiment using the calcium hydroxides as foulants, it is thought that the gas temperature of 700, 850 and 1000 °C is larger than the critical gas temperature and the average fouling factor does not depend much on the gas temperature above 700 °C.

4. Summary and Conclusions

We designed the hot wind tunnel and investigated the effects of position along the fouling probe, flow rate of cooling air, foulant feeding rate and gas temperature on the heat transfer and fouling.

If the foulant is adhered to the fouling probe, the heat transfer rate decreases and the fouling factor increases vary rapidly during an early period of fouling process. As time goes by, the heat transfer rate and fouling factor approach to an equilibrium value, since the amount of the foulant adhered to the fouling probe is approximately equal to that removed from the probe.

Because the amount of foulant adhered to the probe surface has a maximum value at the stagnation point, the fouling factor at the stagnation point has a maximum value. The amount of foulant deposition decreases in the stream-wise direction but increases again due to the re-entrainment of foulant in the wake region. Thus the amount of foulant deposition and fouling factor at $\theta=180°$ are larger than those at $\theta=90°$.

The amount of adhered on the fouling probe and fouling factor increases with flow rate of cooling air and foulant feeding rate. The local fouling factor increases with gas temperature but the average fouling factor does not depend much on the gas temperature above 700°C

Acknowledgments

The authors would like to express their appreciation to the Korea Science and Engineering Foundation (KOSEF-94-0200-07-01-3) for their partial financial supports on this study.

References

Barratt, D. J. and Unsworth, J. F., 1988, "Ash Formation During Pulverized Coal Combustion," *FUEL,* Vol. 67, pp. 1503~1509

Baxter, L. L. and Desollar, R. W., 1993, "A Mechanistic Description of Ash Deposition During Pulverized Coal Combustion: Predictions Compared With Observations," *FUEL,* Vol. 72, pp. 1411~1418

Baxter, L. L., Hencken, K. R. and Harding, N. S., 1990, "The Dynamic Variation of Particle Capture Efficiency During Ash Deposition in Coal-Fired Combustors," *Twenty-Third Symposium (International) on Combustion,* pp. 993~999

Borio, R. W., Goetz, G. J. and Levasseur, A. 1977, "Slagging and Fouling Properties of Coal Ash Deposits as Determined in a Laboratory Test Facility, *Presented at the ASME Winter Annual Meeting,* Atlanta, Georgia.

Gdmundson, J. S., 1981, "Particulate Fouling," *Fouling in Heat Transfer Equipment,* E. F. C. Somerscales and J. G. Knudsen eds., Hemisphere Publishing Company, 357~387, Washington D. C., pp. 357~387.

Ha, M. Y. and Kim K., 1996, "Particulate Two-Phase Flow Analysis for Fouling Prediction," Final report to the Korea Science and Engineering Foundation, KOSEF-94-0200-07-01-3.

Ha, M. Y., Lee, D. R., Ahn, S. P., Kim, K. C., Kim, K. S., Lee, J. K., and Park, H. D., 1996, "Particulate Two-Phase Flow Analysis for Fouling Prediction (I) - Design of Hot Wind Tunnel and Its Performance Experiment," *Transactions of the Korean Society of Mechanical Engineers,* Vol. 20, No. 11, pp. 3695~3705

Kamer, F. R., Zygarlicke, C. J. and Brekke, D. W., 1994, "New Analysis Techniques Help Control Boiler Fouling," *Power Engineering,* pp. 35~38.

Lee, D. H., Lee, B. E., Ha, M. Y., Lim, T. W., Lee, J. H. and Kim, K. S., 1997, "A Theoretical Study of Particulate Deposition on a Tube," *Proceedings of 1997 KSME Fall Annual*

Meeting.

Lister, D. H., 1981, "Corrosion Products in Power Generating Systems," *Fouling in Heat Transfer Equipment,* E. F. C. Somerscales and J. G. Knudsen eds., Hemisphere Publishing Company, Washington, D. C., pp. 135~200

Marner, W. J. and MacDavid, K. S., 1989, "Development of a Gas Side Fouling Measuring Device," *1989 National Heat Transfer Conference HTD-Vol 108,* pp. 305~314.

Nbeal, S. K., 1970, "Deposition of Particles in Turbulence Flow on Channel or Pipe Walls," *Nuclear Science and Engineering,* Vol. 40, pp. 1~11.

Reid, W. T. . 1984, "The Relation of Mineral Composition to Slagging, Fouling and Erosion During and After Combustion," *Prog. Energy Combust.,* Vol. 10, pp. 159~175.

Sohal, M. S., 1993, "Field Testing of a Probe to Measure Fouling in an Industrial Flue Gas Stream," *Heat Transfer Engineering,* Vol. 14, pp. 51~61.

Tulapurkara, E. G. and Bhalla, V. V. K., 1988, "Experimental Investigation of Morel's Method for Wind Tunnel Conditions," *Journal of Fluid Engineering,* Vol. 100, pp. 45~47.

Walsh, P. M., Sarofim, A. F. and Beer, J. M., 1992, "Fouling of Convection Heat Exchangers by Lignitic Coal Ash," *Energy & Fuels,* pp. 709~715.

Walsh, P. M., Sayre, A. N., Loehden, D. O., Monroe, L. S., Beer, J. M., and Sarofim, A. F., 1990, "Deposition of Bituminous Coal Ash on an Isolated Heat Exchanger Tube: Effects of Coal Properties on Deposition Growth," *Prog. Energy Combust.,* Vol. 16, pp. 327~346.

Wenglarz, R. A., 1981, "An Assessment of Deposition in PFBC Power Plant Turbines," *ASME Journal of Engineering for Power,* Vol. 103, pp. 552~560.